Article

Not peer-reviewed version

Excited-State Polarizabilities: A Combined Density Functional Theory and Information-Theoretic Approach Study

Dongbo Zhao , Xin He , Paul W. Ayers * , Shubin Liu *

Posted Date: 7 February 2023

doi: 10.20944/preprints202302.0116.v1

Keywords: density functional theory; information theory; excited-state polarizability; ESIPT (excited-state intramolecular proton transfer)

Article

Excited-State Polarizabilities: A Combined Density Functional Theory and Information-Theoretic Approach Study

Dongbo Zhao [1], Xin He [2], Paul W. Ayers [3,*] and Shubin Liu [4,5,*]

1 Institute of Biomedical Research, Yunnan University, Kunming 650500, P. R. China
2 Qingdao Institute for Theoretical and Computational Sciences, Shandong University, Qingdao 266237, Shandong, P. R. China
3 Department of Chemistry and Chemical Biology, McMaster University, Hamilton, ONL8S 4M1, Canada
4 Research Computing Center, University of North Carolina, Chapel Hill, NC 27599-3420, USA
5 Department of Chemistry, University of North Carolina, Chapel Hill, NC 27599-3290, USA
* Correspondence: ayers@mcmaster.ca and shubin@email.unc.edu

Abstract: Accurate and efficient determination of excited-state polarizabilities (α) is an open problem both experimentally and computationally. Following our previous work, [Phys. Chem. Chem. Phys. **2023**, 25, 2131–2141], where one can employ simple ground-state (S_0) density-related functions from the information-theoretic approach (ITA) to accurately and efficiently evaluate the macromolecular polarizabilities, we aim to predict the lowest excited-state (S_1) polarizabilities in this work. The philosophy is to use density-based functions to depict the excited-state polarizabilities. As a proof-of-principle application, employing 2-(2′-hydroxyphenyl)benzimidazole and its substituents as model systems, we have verified that either with S_0 or S_1 densities as input, ITA quantities can be strongly correlated with the excited-state polarizabilities. When the transition densities are considered, both S_0 and S_1 polarizabilities are in good relationships with some ITA quantities. Furthermore, excitation and emission energies can be predicted based on multivariant linear regression equations of ITA quantities.

Keywords: density functional theory; information theory; excited-state polarizability; ESIPT (excited-state intramolecular proton transfer)

1. Introduction

Molecular polarizability, especially the static electric dipole polarizability (α), is a fundamental physicochemical property. It reflects the change of a molecule's dipole moment in a linear-response manner, as resulted from an external electric field perturbation. [1] The experimental determination of excited-state electro-static properties are mainly the Stark spectroscopy or electronic absorption/emission [2,3] method and the flash photolysis time-resolved microwave-conductivity (FP-TMRC) [4,5] technique.

In classical physics, the polarizability can be approximately obtained in terms of the volume of a system. [6,7] For example, many strong correlations have been observed for both atoms and molecules. [8–16] It is worthwhile to mention that Tkatchenko and Scheffler (TS) [17] proposed to use atomic volumes and atomic polarizabilities to predict the ground-state polarizabilities for small molecules. Recent progress can be found in ref 18. However, its performance for excited-state systems has not been reported.

In quantum mechanics, the polarizability can be obtained by iteratively solving the coupled-perturbed Hartree–Fock (CPHF) equation [19,20] or its Kohn–Sham DFT (density functional theory) counterpart. [21] Of note, this protocol requires a sufficiently large basis set with polarization and diffuse functions and huge computational costs. Note that the computational barriers can be partly overcome by using some linear-scaling methods. [22–24] In addition, machine learning (ML)-based [25–27] methods and a regression-based [28] model have been applied to predict the S_0 polarizabilities. It is worthy to note that the polarizability can be related to the band gap of HOMO

Preprints (www.preprints.org) | NOT PEER-REVIEWED | Posted: 7 February 2023 doi:10.20944/preprints202302.0116.v1

(highest occupied molecular orbital) and LUMO (lowest unoccupied molecular orbital) in an inverse manner. [29–31]

In the literature, only a few studies [32–38] have been reported for the excited-state polarizabilities. This is likely because that accurate predictions of excited-state geometries and molecular properties of large molecules is a tough nut to crack, especially when there are perturbations such as external fields.

Following our previous work where the information-theoretic approach (ITA) quantities are employed to predict the S_0 polarizabilities of both small and large molecules, [39,40] here we aim to predict the S_1 polarizabilities of 2-(2′-hydroxyphenyl)benzimidazole (HBI, **1**) and its derivatives as shown in **Figure 1**. For **1**, it is well-documented [41] that the S_0 (**Figure 1a**) intramolecular proton transfer (IPT) reaction is difficult to take place and the S_1 (**Figure 1b**) or T_1 (triplet, not shown) intramolecular proton transfer (ESIPT) process can easily happens. Thus, in this work, only S_0 and S_1 are considered to reduce the computational cost without compromising the results much. We have found that with the S_0 or S_1 electron densities as input, ITA quantities can be in good correlations with the excited-state polarizabilities. When the transition densities are considered, both S_0 and S_1 polarizabilities can be in good relationships with ITA quantities. Furthermore, excitation and emission energies can be predicted based on multiple linear regression equations of ITA quantities. For the first time, we have applied the ITA quantities to predict the excited-state polarizabilities. It is anticipated that this protocol can be readily applied to condensed-phase systems.

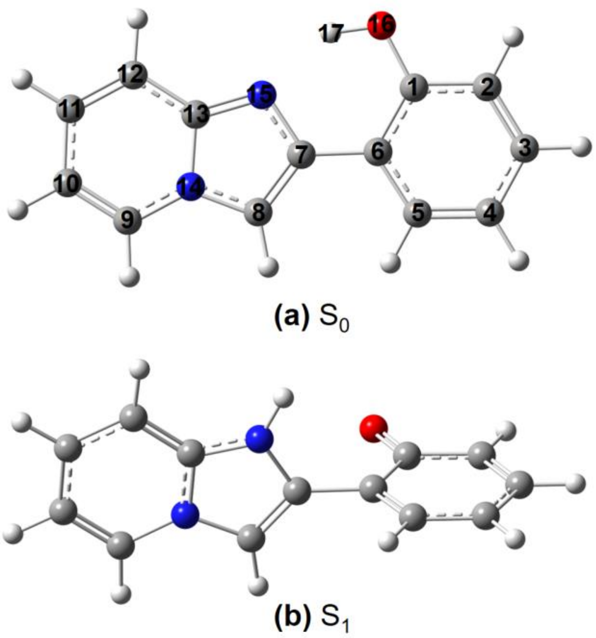

Figure 1. Schematic representation of the (a) ground-state (S_0) and (b) excited-state (S_1) 2-(2′-hydroxyphenyl)benzimidazole (HBI) structure and the atomic numbering. A total of 27 substituted HBI structures are generated, including **1**: HBI, **2**: 3-Br-HBI, **3**: 3-Et_2N-HBI, **4**: 3-HO-HBI, **5**: 3-MeO-HBI, **6**: 4-F-HBI, **7**: 4-Cl-HBI, **8**: 4-Br-HBI, **9**: 4-CN-HBI, **10**: 4-Me-HBI, **11**: 4-MeO-HBI, **12**: 10-Cl-HBI, **13**: 10-Br-HBI, **14**: 10-CN-HBI, **15**: 10-Me-HBI, **16**: 10-CF_3-HBI, **17**: 10-Ph-HBI, **18**: 12-Ph-HBI, **19**: 10-(*p*-MeO-Ph)-HBI, **20**: 10-(*p*-$MeCO_2$-Ph)-HBI, **21**: 12-(*p*-MeO-Ph)-HBI, **22**: 12-(*p*-$MeCO_2$-Ph)-HBI, **23**: 4-Me-10-Cl-HBI, **24**: 4-Me-10-CF_3-HBI, **25**: 10-Ph-12-Ph-HBI, **26**: 2-($CH_2CH_2CH{=}CH_2$)-8-(CH_2CH_2Ph)-HBI, **27**: 2-F-3-F-4-F-5-F-HBI. Color code: hydrogen in white, carbon in grey, nitrogen in blue, and oxygen in red.

2. Results

Shown in **Table 1** are the correlation coefficients (R^2) between the S_0 polarizabilities (α_{iso}) and ITA quantities, molecular volumes, and quadrupole moments, which are obtained at the CAM-B3LYP/6-311+G(d) level. It is clear from **Table 1** that Ghosh–Berkowitz–Parr (GBP) entropy (S_{GBP}),

Preprints (www.preprints.org) | NOT PEER-REVIEWED | Posted: 7 February 2023 doi:10.20944/preprints202302.0116.v1

2nd and 3rd relative Rényi entropy (${}^{r}R_2$ and ${}^{r}R_3$), information gain (I_G), G_1, G_2, and G_3, and quadrupole moments (Θ_{iso}) are in strong linear relationships with α_{iso}, with $R^2 > 0.8$. However, molecular volumes are in only reasonaly good coorelation with α_{iso}, with $R^2 = 0.618$, indicating that it is not a good descriptor of α_{iso}. Of note, the G_3 data have been shown to be strongly correlated with α_{iso} for various systems, among which are 30 planar or quasi-planar bases, [39] 20/40/8000 amino acids/dipeptides/tripeptides, [39] and so on. [40] Also, the Θ_{iso} values can be in good relationship with α_{iso} and its theoretical rational can be found in ref 40. However, a solid and sound theoretical verification between G_3 and α_{iso} is staill lacking. Overall, the strong correlations can serve as an argument that our computational results are convincing.

Table 1. Correlation coefficient (R^2) between the isotropic molecular polarizability (α_{iso}, in Bohr^3) and ITA quantities (in a.u.), molecular volume (Vol, in Bohr^3/mol), and the isotropic quadrupole moment (Θ_{iso}, in a.u.) at S_0.

index	α_{iso}	S_S	I_F	S_{GBP}	${}^{r}R_2$	${}^{r}R_3$	I_G	G_1	G_2	G_3	Vol	Θ_{iso}
1	175.68	96.35	4343.89	746.75	112.64	117.78	1.38	−35.34	24.07	139.78	1715.75	−87.39
2	200.87	20.66	13967.27	973.91	146.61	151.68	1.36	−34.93	23.70	141.74	2073.70	−103.29
3	237.32	142.90	5692.80	1016.86	154.03	161.91	2.10	−50.98	35.00	196.05	2441.40	−115.43
4	182.97	97.74	4793.46	801.56	120.76	126.07	1.45	−34.44	22.49	147.78	1855.73	−91.79
5	197.76	107.94	5045.63	855.45	129.06	135.01	1.60	−39.10	25.75	159.82	1886.74	−95.32
6	175.11	92.94	4917.98	801.81	120.62	125.71	1.37	−34.55	22.69	144.27	1765.67	−93.87
7	188.87	81.70	6524.29	855.22	128.61	133.70	1.37	−34.93	22.13	142.27	1959.26	−100.99
8	197.51	20.60	13967.06	973.87	146.60	151.67	1.36	−34.95	23.67	141.84	1850.09	−101.48
9	194.07	102.37	4928.42	829.28	124.78	130.18	1.46	−36.68	23.12	151.22	1897.41	−106.85
10	189.36	106.46	4595.48	800.72	120.93	126.64	1.53	−39.13	25.97	150.98	1931.31	−93.18
11	194.81	107.96	5045.77	855.48	129.06	135.02	1.60	−39.13	23.71	159.81	1994.38	−95.26
12	191.68	81.72	6524.35	855.23	128.60	133.66	1.36	−34.98	22.67	142.29	1957.16	−105.11
13	200.29	20.66	13967.37	973.93	146.60	151.67	1.36	−35.01	22.86	141.85	1980.91	−111.96
14	198.88	102.42	4928.71	829.32	124.77	130.16	1.45	−36.79	23.62	151.19	1696.49	−112.11
15	190.18	106.46	4595.43	800.71	120.93	126.64	1.53	−39.12	24.61	151.02	1842.17	−94.41
16	191.22	96.42	6318.70	965.73	144.80	150.24	1.46	−37.81	23.40	165.13	2064.71	−117.92
17	255.95	135.18	5826.22	1017.73	153.69	160.90	1.92	−52.71	36.65	192.16	2401.28	−125.79
18	246.58	135.11	5826.00	1017.67	153.68	160.90	1.92	−52.74	36.93	192.52	2494.60	−119.81
19	277.67	146.79	6528.00	1126.45	170.10	178.13	2.14	−56.48	38.53	212.18	2819.11	−137.35
20	295.24	153.19	7225.20	1222.09	184.32	192.76	2.25	−58.90	39.85	226.76	2761.18	−154.13
21	268.01	146.71	6527.76	1126.38	170.10	178.12	2.14	−56.47	39.11	212.53	2467.93	−128.04
22	283.05	153.12	7225.00	1222.03	184.32	192.76	2.25	−58.93	39.71	227.00	2913.80	−139.45
23	205.46	91.83	6775.95	909.20	136.89	142.52	1.51	−38.70	26.44	153.26	1963.41	−110.94
24	205.03	106.53	6570.28	1019.70	153.09	159.11	1.61	−41.55	26.57	176.20	2201.13	−123.83
25	327.20	173.93	7308.31	1288.65	194.73	204.01	2.46	−70.08	50.17	244.74	3066.91	−156.33
26	320.10	190.84	7330.19	1328.47	201.30	211.70	2.76	−74.61	52.80	255.30	3332.26	−160.67
27	175.19	82.72	6640.05	966.86	144.50	149.36	1.31	−32.94	20.03	158.50	3218.41	−108.98
R^2	1.000	0.581	0.005	0.859	0.868	0.883	0.927	0.959	0.955	0.931	0.618	0.869

Collected in **Table 2** are the S_1 polarizabilities, the S_1 ITA quantities including Shannon entropy (S_S), Fisher information (I_F), 2nd and 3rd relative Rényi entropy (${}^{r}R_2$ and ${}^{r}R_3$), G_2 and G_3, molecular volumes (Vol), and quadrupole moments (Θ_{iso}), which are obtained at the TD-CAM-B3LYP/6-311+G(d) level. Also given in **Table 2** are the correlation coefficients (R^2) between the S_1 polarizabilities and other quantities at S_1. Note that some ITA quantities, well-defined at S_0, are numerically ill-behaved at S_1 and thus missing. One can see that ${}^{r}R_2$, ${}^{r}R_3$, G_2, G_3, Vol, and Θ_{iso} are in good correlations with α_{iso} at S_1, with $R^2 > 0.8$. It is intriguing to note that at S_1, G_3 is still in good correlation with α_{iso}. This is the first time to observe such a phenomenon. However, admittedly, the theoretical foundation lags behind the numerical evidence introduced in this work. Moreover, we have found that for Vol, the correlation

 doi:10.20944/preprints202302.0116.v1

coefficient is much stronger at S_1 (0.908) than that at S_0 (0.618). One possible reason is that the excited-state relaxation expands the volume and polarizability space. Finally, one can discover in Column 4 of I_F, **2**, **8**, and **13** seem to have abnormal values compared with the others. They are all Br-containing, indicating that there may be some regions for heavy atoms where density gradients are numerically ill-behaved at S_1. Similar results can also be observed for I_F at S_0 (see **Table 1**). Overall, we have unraveled that excited-state densities and molecular properties are mutually entangled.

Table 2. Correlation coefficient (R^2) between the isotropic molecular polarizability (α_{iso}, in Bohr^3) and ITA quantities (in a.u.), molecular volume (Vol, in Bohr^3/mol), and the isotropic quadrupole moment (Θ_{iso}, in a.u.) at S_1.

index	α_{iso}	S_S	I_F	$^rR_2$	$^rR_3$	G_2	G_3	Vol	Θ_{iso}
1	166.08	96.94	4345.68	112.73	118.02	23.88	138.16	1784.17	–89.93
2	189.81	21.28	13969.19	146.67	151.87	23.61	140.08	1956.89	–114.26
3	224.23	143.51	5694.61	154.12	162.16	34.15	194.24	2519.29	–126.71
4	174.81	98.36	4795.23	120.83	126.27	22.33	146.07	1862.89	–96.38
5	187.84	108.57	5047.40	129.14	135.22	25.53	158.13	1983.35	–101.96
6	166.88	93.55	4919.65	120.68	125.87	22.56	142.61	1809.41	–97.69
7	182.88	82.29	6525.95	128.66	133.83	23.33	140.53	1948.71	–105.58
8	188.20	21.19	13968.88	146.65	151.80	22.97	140.28	1945.05	–110.07
9	182.03	103.04	4930.44	124.83	130.34	24.17	149.51	1945.30	–110.22
10	178.88	107.05	4597.05	121.02	126.88	26.58	149.31	1919.82	–96.99
11	182.81	108.54	5047.21	129.14	135.22	25.57	158.15	1992.00	–99.73
12	178.54	82.29	6526.00	128.69	133.90	23.14	140.43	1905.76	–103.35
13	186.41	21.24	13968.99	146.69	151.92	23.40	139.90	1961.97	–105.81
14	185.73	102.96	4930.10	124.85	130.37	24.33	149.38	1959.21	–111.23
15	179.03	107.06	4597.29	121.01	126.87	26.78	149.25	1938.52	–94.93
16	178.64	96.95	6320.18	144.88	150.45	23.97	163.21	2040.58	–111.79
17	240.42	135.77	5827.95	153.76	161.09	36.81	190.49	2466.79	–117.96
18	253.40	135.66	5827.52	153.75	161.08	36.75	190.81	2411.54	–120.97
19	260.31	147.38	6529.77	170.17	178.31	39.03	210.40	2664.07	–124.40
20	280.48	153.76	7226.84	184.39	192.94	40.08	225.02	2822.78	–136.33
21	267.99	147.29	6529.43	170.17	178.33	38.50	210.79	2665.63	–128.47
22	327.99	153.50	7225.08	184.32	192.78	39.42	226.35	2798.30	–138.46
23	190.90	92.40	6777.37	136.99	142.77	25.46	151.82	2091.13	–110.61
24	191.30	107.05	6571.54	153.18	159.32	26.69	174.50	2213.23	–119.08
25	331.10	174.16	7307.99	194.72	204.02	48.71	244.76	3050.07	–168.67
26	309.58	191.50	7332.09	201.39	211.92	53.05	253.29	3379.72	–164.60
27	190.21	83.28	6640.35	144.47	149.29	19.82	157.57	1894.17	–115.25
R^2	1.000	0.560	0.004	0.861	0.874	0.884	0.917	0.908	0.831

Now we have shown that ITA quantities can be correlated with α_{iso} either at S_0 or S_1. It is natural to ask if one can use ITA quantities at S_0 to predict α_{iso} at S_1. The answer is definitely yes! In Table 3, We have tabulated the correlation coefficients (R^2) between the α_{iso} values at S_1 and ITA quantities, molecular volumes, and quadrupole moments at S_0 as introduced in Table 1. More details can be found in Table S1. Except Shannon entropy (S_S), Fisher information (I_F), and molecular volumes (Vol), the other quantities at S_0 are in good relationships with α_{iso} at S_1, with $R^2 > 0.8$. Moving forward, we ask if one can use the transition density (matrix) as input for ITA quantities to correlate with α_{iso} either at S_0 or S_1. The answer is again yes! Shown in Table 4 are the strong correlations between α_{iso} either at S_0 or S_1 and ITA quantities with the transition density matrix. Except Shannon entropy (S_S) and Fisher information (I_F), the other ITA quantities are in strong correlations with α_{iso} either at S_0 or S_1, with $R^2 > 0.8$. Implication of this part is straightforward that electron-density-based quantities can be used to predict the excited-state properties, such as molecular polarizabilities.

 doi:10.20944/preprints202302.0116.v1

Table 3. Correlation coefficient (R^2) between the α_{iso}@S_1, and α_{iso}@S_0, ITA quantities@S_0, Vol@S_0, and Θ_{iso}@S_0.

	α_{iso}	S_S	I_F	S_{GBP}	${}^{r}R_2$	${}^{r}R_3$
R^2	0.941	0.561	0.004	0.855	0.862	0.874
	I_G	G_1	G_2	G_3	Vol	Θ_{iso}
R^2	0.876	0.906	0.896	0.914	0.688	0.814

Table 4. Correlation coefficient (R^2) between the α_{iso}@S_0/S_1 and ITA quantities based on the transition density matrix .

R^2	S_S	I_F	S_{GBP}	${}^{r}R_2$	${}^{r}R_3$	I_G	G_1	G_2	G_3
α_{iso}@S_0	0.580	0.005	0.859	0.868	0.883	0.927	0.959	0.955	0.932
α_{iso}@S_1	0.561	0.004	0.855	0.862	0.874	0.873	0.907	0.897	0.914

Next, we will compare the α_{iso} data (either at S_0 or S_1) predicted by the TS formulas as with conventional results as reference. Employing the original Tkatchenko–Scheffler (TS) formula [17] on top of Becke [42] or Hirshfeld [43] partitions, the α_{iso} data (either at S_0/S_1) are either strongly underestimated or overestimated, with MUE(%) up to –24.90/–21.21 and 6.62/10.82, respectively, as shown in Table 5. It is found that a mean value can reduce the MSE(%) to 16.00/15.23. Moreover, with the new TS formula, [18] the results are not improved but worsened as shown in Table 6. Taken together, we have found that the TS formulas have large room to improve in predicting the S_1 polarizabilities.

Table 5. Comparison of molecular polarizabilities (α_{iso}) at S_0/S_1 predicted by the original TS formula with conventional data as reference.

index	Ground-state (S_0)			Excited-state (S_1)		
	Becke	Hirshfeld	avg.	Becke	Hirshfeld	avg.
1	119.84	176.99	148.41	121.05	176.63	148.84
2	228.99	281.15	255.07	228.53	279.36	253.95
3	167.92	250.19	209.05	169.26	249.87	209.56
4	122.82	182.28	152.55	124.20	182.08	153.14
5	132.97	197.56	165.27	134.35	197.34	165.84
6	119.40	177.07	148.24	120.98	177.15	149.06
7	170.42	224.86	197.64	170.23	223.53	196.88
8	229.52	281.83	255.67	227.91	279.02	253.46
9	129.98	189.98	159.98	131.48	190.06	160.77
10	129.77	192.41	161.09	131.17	192.26	161.72
11	132.81	197.40	165.11	134.35	197.35	165.85
12	169.65	224.32	196.98	172.04	224.59	198.32
13	227.44	279.92	253.68	231.41	281.70	256.56
14	130.12	190.12	160.12	131.17	189.61	160.39
15	129.85	192.48	161.16	131.10	192.26	161.68
16	130.63	194.40	162.51	131.24	193.58	162.41
17	167.50	248.17	207.83	168.68	247.78	208.23
18	167.20	248.13	207.66	168.36	247.93	208.14
19	180.67	268.74	224.70	181.79	268.33	225.06
20	190.15	282.83	236.49	191.24	282.39	236.82
21	180.36	268.73	224.55	181.54	268.42	224.98
22	189.86	282.78	236.32	190.76	283.63	237.19
23	179.61	239.76	209.69	182.19	240.24	211.21
24	140.56	209.82	175.19	141.35	209.19	175.27
25	214.86	319.29	267.08	214.84	321.13	267.99
26	226.85	337.95	282.40	228.26	337.38	282.82

 doi:10.20944/preprints202302.0116.v1

27	119.65	177.97	148.81	121.63	179.51	150.57
MUE (%)[a]	–24.90	6.62	–9.14	–21.21	10.82	–5.19
MSE (%)[b]	28.14	8.10	16.00	26.07	12.63	15.23

[a]**MUE**: mean unsigned error. [b]**MSE**: mean signed error.

Table 6. Comparison of molecular polarizabilities (α_{iso}) at S_0/S_1 predicted by the new TS formula with conventional data as reference.

index	Ground-state (S_0)			Excited-state (S_1)		
	Becke	Hirshfeld	avg.	Becke	Hirshfeld	avg.
1	119.84	176.99	148.41	121.05	176.63	148.84
2	228.99	281.15	255.07	228.53	279.36	253.95
3	167.92	250.19	209.05	169.26	249.87	209.56
4	122.82	182.28	152.55	124.20	182.08	153.14
5	132.97	197.56	165.27	134.35	197.34	165.84
6	119.40	177.07	148.24	120.98	177.15	149.06
7	170.42	224.86	197.64	170.23	223.53	196.88
8	229.52	281.83	255.67	227.91	279.02	253.46
9	129.98	189.98	159.98	131.48	190.06	160.77
10	129.77	192.41	161.09	131.17	192.26	161.72
11	132.81	197.40	165.11	134.35	197.35	165.85
12	169.65	224.32	196.98	172.04	224.59	198.32
13	227.44	279.92	253.68	231.41	281.70	256.56
14	130.12	190.12	160.12	131.17	189.61	160.39
15	129.85	192.48	161.16	131.10	192.26	161.68
16	130.63	194.40	162.51	131.24	193.58	162.41
17	167.50	248.17	207.83	168.68	247.78	208.23
18	167.20	248.13	207.66	168.36	247.93	208.14
19	180.67	268.74	224.70	181.79	268.33	225.06
20	190.15	282.83	236.49	191.24	282.39	236.82
21	180.36	268.73	224.55	181.54	268.42	224.98
22	189.86	282.78	236.32	190.76	283.63	237.19
23	179.61	239.76	209.69	182.19	240.24	211.21
24	140.56	209.82	175.19	141.35	209.19	175.27
25	214.86	319.29	267.08	214.84	321.13	267.99
26	226.85	337.95	282.40	228.26	337.38	282.82
27	119.65	177.97	148.81	121.63	179.51	150.57
MUE (%)[a]	–28.40	6.77	–10.82	–24.74	11.05	–6.84
MSE (%)[b]	39.16	15.48	26.74	37.89	16.21	26.41

[a]**MUE**: mean unsigned error. [b]**MSE**: mean signed error.

Finally, we have found that both excitation and emission energies can be predicted on top of multiple linear regression equations of ITA quantities. For example, one can use the transition density matrix as input for ITA quantities to correlate with the excitation energies. Similarly, if the S_1 densities are used for ITA quantities, the emission energies can be predicted. Based on the two regression equations,

$\lambda_{fit} = 0.32{*}S_S + 0.0027{*}I_F - 0.31{*}S_{GBP} - 0.85{*}{}^rR_2 + 2.87{*}{}^rR_3 - 27.99{*}I_G + 0.33{*}G_1 - 0.050{*}G_2 + 0.0099{*}G_3$, and

$\lambda_{fit} = 0.085{*}S_S + 0.00088{*}I_F + 1.36{*}{}^rR_2 - 1.42{*}{}^rR_3 - 0.080{*}G_2 + 0.038{*}G_3$,

we have obtained that the **MUEs** (mean unsigned error) and the **MSEs** (mean signed error) are –0.04/0.20 eV and 0.00/0.22 eV for excitation and emission energies, respectively. This indicates that the inaccuracy of this protocol is comparable to that of underlying approximations of DFT. [44,45]

3. Discussion

To accurately and efficiently predict the excited-state polarizabilities is an ongoing issue. Solving standard CPHF/CPKS equations are computationally intensive and the computational costs can be intractable for macromolecular systems. Other algorithms and models available in the literature are normally concerned with the ground-state polarizabilities. Within this context; we proposed to apply some density-based ITA quantities to correlate with α_{iso} at S_0/S_1. This is inspired by our previous work on predicting the ground-state polarizabilities for small and macromolecular systems. Our tentative results have shown that the protocol should be a promising theoretical tool. More systems along this line need to be considered to make this protocol more robust and applicable. We have to point out when the system under study becomes larger and larger; the molecular wavefunctions (thus electron density) are a tough nut to crack; sometimes computationally intractable. Under these circumstances; we have to resort to linear-scaling electronic structure methods; such as GEBF (generalized energy-based fragmentation method), [46–49] where only small subsystems of a few atoms or groups are treated.

Next, we will look into the TS method, as mentioned previously. We have already found that based upon the Hirshfeld or Becke partition scheme, the original TS formula has an unsatisfactory performance either by overestimating or underestimating the S_1 polarizabilities. Apparent reduction of the deviations can be obtained by averaging the two sets of results. The reason behind is unclear at the moment. From the original formula,

$$\alpha_{\mathrm{mol}}^{\mathrm{TS-old}} = \sum_{\mathrm{A}} \alpha_{\mathrm{A}}^{\mathrm{eff}} = \sum_{\mathrm{A}} \alpha_{\mathrm{A}}^{\mathrm{free}} \left(\frac{V_{\mathrm{A}}^{\mathrm{eff}}}{V_{\mathrm{A}}^{\mathrm{free}}} \right)$$

one can easily argue that the weights $\left(\frac{V_{\mathrm{A}}^{\mathrm{eff}}}{V_{\mathrm{A}}^{\mathrm{free}}} \right)$ may be the root cause of its poor performance, mainly because the atomic polarizabilities $\alpha_{\mathrm{A}}^{\mathrm{free}}$ are experimentally determined and computationally verified, as summarized in ref 50. In the same spirit, a revised TS formula,

$$\alpha_{\mathrm{mol}}^{\mathrm{TS-new}} = \sum_{\mathrm{A}} \alpha_{\mathrm{A}}^{\mathrm{eff}} = \sum_{\mathrm{A}} \alpha_{\mathrm{A}}^{\mathrm{free}} \left(\frac{V_{\mathrm{A}}^{\mathrm{eff}}}{V_{\mathrm{A}}^{\mathrm{free}}} \right)^{4/3}$$

has witnessed improved performance of predicting the S_0 polarizabilities. However, its predicting power has been shown to be far from satisfactory for macromolecules. In this work, we further corroborate that both the original and new TS formulas fail to give a satisfactory description of the S_1 polarizability. This indicates that the two formulas are oversimplified and may be system-dependent. Overall, the volume-based are inferior to the density-based ITA quantities.

4. Materials and Methods

4.1. Information-Theoretic Approach Quantities

Shannon entropy S_S [51] and Fisher information I_F [52] are two cornerstone quantities in information theory. They are defined as Equations (1) and (2), respectively.

$$S_{\mathrm{S}} = -\int \rho(\mathbf{r}) \ln \rho(\mathbf{r}) d\mathbf{r} \quad (1$$

$$I_{\mathrm{F}} = \int \frac{|\nabla \rho(\mathbf{r})|^2}{\rho(\mathbf{r})} d\mathbf{r} \quad (2$$

where $\rho(\mathbf{r})$ is the electron density and $\nabla\rho(\mathbf{r})$ is the density gradient. The physical picture of S_{S} and I_{F} is clear; the former measures the spatial delocalization of the electron density and the latter gauges the sharpness or localization of the same.

Except the total density, more ingredients, such as kinetic-energy density, can be used to defined an ITA quantity. With both the electron density and the kinetic energy density, Ghosh, Berkowitz, and Parr developed a formula for entropy (S_{GBP}), [53]

$$S_{\mathrm{GBP}} = -\int \frac{3}{2} k\rho(\mathbf{r}) \left[c + \ln \frac{t(\mathbf{r};\rho)}{t_{\mathrm{TF}}(\mathbf{r};\rho)} \right] d\mathbf{r} \tag{3}$$

where $t(\mathbf{r}; \rho)$ and $t_{\mathrm{TF}}(\mathbf{r}; \rho)$ represent the non-interacting and Thomas–Fermi (TF) kinetic energy density, respectively. Here k, c, and c_{K} are three constants [k, the Boltzmann constant, $c = (5/3) + \ln(4\pi c_{\mathrm{K}}/3)$, and $c_{\mathrm{K}} = (3/10)(3\pi^2)^{2/3}$]. Full integration of the kinetic energy density $t(\mathbf{r}; \rho)$ leads to the total kinetic energy T_{S} via

$$\int t(\mathbf{r};\rho) d\mathbf{r} = T_{\mathrm{S}} \tag{4}$$

while $t(\mathbf{r}; \rho)$ can be obtained from the canonical orbital densities,

$$t(\mathbf{r};\rho) = \sum_i \frac{1}{8} \frac{\nabla\rho_i \cdot \nabla\rho_i}{\rho_i} - \frac{1}{8}\nabla^2\rho \tag{5}$$

and $t_{\mathrm{TF}}(\mathbf{r}; \rho)$ is simply cast in terms of $\rho(\mathbf{r})$,

$$t_{\mathrm{TF}}(\mathbf{r};\rho) = c_{\mathrm{K}}\rho^{5/3}(\mathbf{r}) \tag{6}$$

Of note, the kinetic-energy density can differ in its form, thus can be used in different contexts. [54–61] But, S_{GBP} satisfies the maximum-entropy requirement from a mathematical viewpoint. [53]

Moving forward, some ITA quantities have been introduced for chemical reactions. As new reactivity descriptors in conceptual density functional theory (CDFT), [62–65] one example is relative Rényi entropy [66] of order n

$$R_n^r = \frac{1}{n-1} \ln \left[\int \frac{\rho^n(\mathbf{r})}{\rho_0^{n-1}(\mathbf{r})} d\mathbf{r} \right] \tag{7}$$

Information gain [67] (also called Kullback–Leibler divergence or relative Shannon entropy) I_{G} is expressed as follows,

$$I_{\mathrm{G}} = \int \rho(\mathbf{r}) \ln \frac{\rho(\mathbf{r})}{\rho_0(\mathbf{r})} d\mathbf{r} \tag{8}$$

In Equations (7) and (8), $\rho_0(\mathbf{r})$ and $\rho(\mathbf{r})$ satisfy the same normalization condition, and $\rho_0(\mathbf{r})$ denotes the reference-state density.

Recently, [68] one of the present authors proposed three functions G_1, G_2, and G_3, at both atomic and molecular levels. They are defined as below:

$$G_3 = \sum_{\mathrm{A}} \int \rho_{\mathrm{A}}(\mathbf{r}) [\nabla \ln \frac{\rho_{\mathrm{A}}(\mathbf{r})}{\rho_{\mathrm{A}}^0(\mathbf{r})}]^2 d\mathbf{r} \tag{9}$$

$$G_1 = \sum_{\mathrm{A}} \int \nabla^2 \rho_{\mathrm{A}}(\mathbf{r}) \frac{\rho_{\mathrm{A}}(\mathbf{r})}{\rho_{\mathrm{A}}^0(\mathbf{r})} d\mathbf{r} \tag{10}$$

$$G_2 = \sum_{\mathrm{A}} \int \rho_{\mathrm{A}}(\mathbf{r}) \left[\frac{\nabla^2 \rho_{\mathrm{A}}(\mathbf{r})}{\rho_{\mathrm{A}}(\mathbf{r})} - \frac{\nabla^2 \rho_{\mathrm{A}}^0(\mathbf{r})}{\rho_{\mathrm{A}}^0(\mathbf{r})} \right] d\mathbf{r} \tag{11}$$

Equations (9)–(11) have been theoretically derived, numerically verified, and have witnessed many applications, as can be found in refs 39, 40, 68, and 69. It is one of our major achievements during the past decade, when we aimed to glue the density functional theory and information theory together in a seamless manner. Because these two theories both can have as electron density as input. Our recent progress along this line can be found in two reviews. [70,71] As another prominent example, we have applied the ITA to appreciate homochirality. [72,73]

Finally, the Hirshfeld's stockholder approach [43,74–77] is often introduced to partition atoms in a molecule in the literature, as defined in Equation (12),

Preprints (www.preprints.org) | NOT PEER-REVIEWED | Posted: 7 February 2023 doi:10.20944/preprints202302.0116.v1

$$\rho_{\mathrm{A}}(\mathbf{r}) = \omega_{\mathrm{A}}(\mathbf{r})\rho(\mathbf{r}) = \frac{\rho_{\mathrm{A}}^{0}(\mathbf{r})(\mathbf{r}-\mathbf{R}_{\mathrm{A}})}{\sum_{\mathrm{B}}\rho_{\mathrm{B}}^{0}(\mathbf{r}-\mathbf{R}_{\mathrm{A}})}\rho(\mathbf{r}) \quad (12$$

Here, $\rho_{\mathrm{A}}(\mathbf{r})$ is the atomic Hirshfeld density, $\omega_{\mathrm{A}}(\mathbf{r})$ is a sharing function, $\rho_{\mathrm{B}}^{0}(\mathbf{r}-\mathbf{R}_{\mathrm{A}})$ is the atomic density of B centered at $\mathbf{R}_{\mathrm{A}}$. The sum over all the free atom densities, typically spherically averaged S_0 atomic densities, is normally termed the promolecular density. The Stockholder approach is natural in the context of ITA because it is also based on information-theoretic arguments. Alternative partitioning schemes include Becke's fuzzy atom approach [44] and Bader's zero-flux atoms-in-molecules (AIM) method. [78]

4.2. Computational Details

All density functional theory (DFT) calculations were performed with the Gaussian 16 [79] package. Default options include ultrafine integration grids and tight self-consistent field convergence, which are adopted to eliminate numerical noises. The ground- and excited-state structural relaxation was fully carried out at the CAM-B3LYP/6-311+G(d) [80,81] and TD-CAM-B3LYP/6-311+G(d) [80,81,82–84] level, respectively, for 27 molecular systems, as shown in **Figure 1**. The optimized atomic Cartesian coordinates are supplied in the Supplementary Materials. Subsequent harmonic vibrational frequency calculations were executed at the same level and no imaginary frequencies were observed by direct visual inspection. The isotropic polarizabilities [α_{iso} = (α_{xx} + α_{yy} + α_{zz})/3] and isotropic quadrupole moments [Θ_{iso} = (Θ_{xx} + Θ_{yy} + Θ_{zz})/3], molecular volumes (at 0.001 e/Bohr^3 contour surface of electronic density), and molecular wavefunctions were obtained at the CAM-B3LYP/6-311+G(d) level. The Multiwfn 3.8 [85] program was utilized to calculate all ITA quantities at S_0 and S_1 by using the checkpoint or wavefunction file as the input. The stockholder Hirshfeld partition scheme of atoms in molecules was employed when atomic contributions were concerned. The reference-state density was the neutral atom calculated at the same level of theory as molecules.

Supplementary Materials: The following supporting information can be downloaded at Preprints.org, Excited-state ITA quantities with the transition density matrix as input, the optimized Cartesian coordinates of all systems (S_0 and S_1).

Author Contributions: Conceptualization, S.L. and D.Z.; data curation, D.Z. and X.H.; formal analysis, D.Z. and X.H.; funding acquisition, D.Z.; project administration, S.L. and D.Z.; supervision, S.L. and D.Z.; writing—original draft, D.Z.; writing—review and editing, S.L. and D.Z. All authors have read and agreed to the published version of the manuscript.

Funding: This work was supported by the start-up funding of Yunnan University and the Yunnan Fundamental Research Projects (grant NO. 202101AU070012).

Institutional Review Board Statement: Not applicable.

Informed Consent Statement: Not applicable.
Data Availability Statement: Data is contained within the article.

Acknowledgments: Pratim K. Chattaraj is acknowledged for this invitation.

Conflicts of Interest: The authors declare no conflict of interest.

References

1. Buckingham, A.D. Polarizability and hyperpolarizability. Phil. Trans. R. Soc. Lond. A **1979**, *293*, 239–248.
2. Liess, M.; Jeglinski, S.; Vardeny, Z.; Ozaki, M.; Yoshino, K.; Ding, Y.; Barton, T. Electroabsorption Spectroscopy of Luminescent and Nonluminescent π-Conjugated Polymers. Phys. Rev. B: Condens. Matter Mater. Phys. **1997**, *56*, 15712–15724.
3. Ponder, M.; Mathies, R. Excited-State Polarizabilities and Dipole Moments of Diphenylpolyenes and Retinal. J. Phys. Chem. **1983**, *87*, 5090–5098.
4. Gelinck, G.H.; Piet, J.J.; Wegewijs, B.R.; Mu¨llen, K.; Wildeman, J.; Hadziioannou, G.; Warman, J.M. Measuring the Size of Excitons on Isolated Phenylene-Vinylene Chains: From Dimers to Polymers. Phys. Rev. B: Condens. Matter Mater. Phys. **2000**, *62*, 1489–1491.

5. De Haas, M.P.; Warman, J.M. Photon-Induced Molecular Charge Separation Studied by Nanosecond Time-Resolved Microwave Conductivity. Chem. Phys. **1982**, *73*, 35–53.
6. Condon, E.U. in *Handbook of Physics*, ed. Condon, E.U. and Odishaw, H. McGraw-Hill, New York, 1958, pp. 4–22.
7. Jackson, J.D. *Classical Electrodynamics*, Wiley, New York, 2nd edn, 1975, pp. 60–62.
8. Dmitrieva, I.K.; Plindov, G.I. Dipole Polarizability, Radius and Ionization Potential for Atomic Systems. Phys. Scr. **1983**, *27*, 402.
9. Gough, K.M. Theoretical analysis of molecular polarizabilities and polarizability derivatives in hydrocarbons. J. Chem. Phys. **1989**, *91*, 2424–2432.
10. Laidig, K.E.; Bader, R.F.W. Properties of atoms in molecules: Atomic polarizabilities. J. Chem. Phys. **1990**, *93*, 7213–7224.
11. Brinck, T.; Murray, J.S.; Politzer, P. Polarizability and volume. J. Chem. Phys. **1993**, *98*, 4305–4306.
12. Politzer, P.; Jin, P.; Murray, J.S. Atomic polarizability, volume and ionization energy. J. Chem. Phys. **2002**, *117*, 8197–8202.
13. Blair, S.A.; Thakkar, A.J. Relating polarizability to volume, ionization energy, electronegativity, hardness, moments of momentum, and other molecular properties. J. Chem. Phys. **2014**, *141*, 074306.
14. Blair, S.A.; Thakkar, A.J. Additive models for the molecular polarizability and volume. Chem. Phys. Lett. **2014**, *610–611*, 163–166.
15. Miller, K.J. Additivity Methods in Molecular Polarizability. J. Am. Chem. Soc. **1990**, *112*, 8533–8542.
16. Miller, K.J. Calculation of the Molecular Polarizability Tensor. J. Am. Chem. Soc. **1990**, *112*, 8543–8551.
17. Tkatchenko, A.; Scheffler, M. Accurate Molecular van der Waals Interactions from Ground-State Electron Density and Free-Atom Reference Data. Phys. Rev. Lett. **2009**, *102*, 073005.
18. Szabó, P.; Góger, S.; Charry, J.; Karimpour, M.R.; Fedorov, D.V.; Tkatchenko, A. Four-Dimensional Scaling of Dipole Polarizability in Quantum Systems. Phys. Rev. Lett. **2022**, *128*, 070602.
19. McWeeny, R. Some recent advances in density matrix theory. Rev. Mod. Phys. **1960**, *32*, 335–369.
20. Langhoff, W.; Karplus, M.; Hurst, R.P. Approximations to Hartree—Fock Perturbation Theory. J. Chem. Phys. **1966**, *44*, 505–514.
21. Colwell, S.M.; Murray, C.W.; Handy, N.C.; Amos, R.D. The determination of hyperpolarisabilities using density functional theory. Chem. Phys. Lett, **1993**, *210*, 261–268.
22. Collins, M.A.; Bettens, R.P. Energy-Based Molecular Fragmentation Methods. Chem. Rev. **2015**, *115*, 5607–5642.
23. Niklasson, A.M.; Challacombe, M. Density Matrix Perturbation Theory. Phys. Rev. Lett. **2004**, *92*, 193001.
24. Weber, V.; Niklasson, A.M.N.; Challacombe, M. Ab Initio Linear Scaling Response Theory: Electric Polarizability by Perturbed Projection. Phys. Rev. Lett. **2004**, *92*, 193002.
25. Grisafi, A.; Wilkins, D.M.; Csányi, G.; Ceriotti, M. Symmetry-Adapted Machine Learning for Tensorial Properties of Atomistic Systems. Phys. Rev. Lett. **2018**, *120*, 036002.
26. Wilkins, D.M.; Grisafi, A.; Yang, Y.; Lao, K.U.; DiStasio, R.A., Jr.; Ceriotti, M. Accurate molecular polarizabilities with coupled cluster theory and machine learning. Proc. Natl. Acad. Sci. U.S.A. **2019**, *116*, 3401–3406.
27. Nguyen, V.H.A.; Lunghi, A. Predicting tensorial molecular properties with equivariant machine learning models. Phys. Rev. B **2022**, *105*, 165131.
28. Amin, M.; Samy, H.; Küpper, J. Robust and Accurate Computational Estimation of the Polarizability Tensors of Macromolecules. J. Phys. Chem. Lett. **2019**, *10*, 2938–2943.
29. Unsöld, A. Quantentheorie des Wasserstoffmolekülions und der Born-Landéschen Abstoßungskräfte, Z. Physik **1927**, *43*, 563–574.
30. Simón-Manso, Y.; Fuentealba, P. On the Density Functional Relationship between Static Dipole Polarizability and Global Softness. J. Phys. Chem. A **1998**, *102*, 2029–2032.
31. Ayers, P.W. The physical basis of the hard/soft acid/base principle. Faraday Discuss. **2007**, *135*, 161–190.
32. Grozema, F.C.; Telesca, R.; Jonkman, H.T.; Siebbeles, L.D.A.; Snijders, J.G. Excited State Polarizabilities of Conjugated Molecules Calculated Using Time Dependent Density Functional Theory. J. Chem. Phys. **2001**, *115*, 10014–10021.
33. Improta, R.; Ferrante, C.; Bozio, R.; Barone, V. The Polarizability in Solution of Tetra-Phenyl-Porphyrin Derivatives in Their Excited Electronic States: A PCM/TD-DFT Study. Phys. Chem. Chem. Phys. **2009**, *11*, 4664–4673.
34. Van Der Horst, J.W.; Bobbert, P.A.; De Jong, P.H.L.; Michels, M.A.J.; Siebbeles, L.D.A.; Warman, J.M.; Gelinck, G.H.; Brocks, G. Predicting Polarizabilities and Lifetimes of Excitons on Conjugated Polymer Chains. Chem. Phys. Lett. **2001**, *334*, 303–308.
35. Hinchliffe, A.; Soscún, H.J. Ab Initio Studies of the Dipole Moment and Polarizability of Azulene in Its Ground and Excited Singlet States. Chem. Phys. Lett. **2005**, *412*, 365–368.
36. Christiansen, O.; Hättig, C.; Jørgensen, P. Ground and Excited State Polarizabilities and Dipole Transition Properties of Benzene from Coupled Cluster Response Theory. Spectrochim. Acta, Part A **1999**, *55*, 509–524.

37. Ye, J.F.; Chen, H.; Note, R.; Mizuseki, H.; Kawazoe, Y. Excess Polarizabilities Upon Excitation from the Ground State to the First Dipole-Allowed Excited State of Diphenylpolyenes. Int. J. Quantum Chem. **2007**, *107*, 2006–2014.
38. Orian, L.; Pilot, R.; Bozio, R. In Silico Stark Effect: Determination of Excited-State Polarizabilities of Squaraine Dyes. J. Phys. Chem. A **2017**, *121*, 1587−1596.
39. Zhao, D.B.; Liu, S.B.; Chen, D.H. A Density Functional Theory and Information-Theoretic Approach Study of Interaction Energy and Polarizability for Base Pairs and Peptides. Pharmaceuticals **2022**, *15*, 938.
40. Zhao, D.B.; Zhao, Y.L.; He, X.; Ayers, P.W.; Liu, S.B. Efficient and accurate density-based prediction of macromolecular polarizabilities. Phys. Chem. Chem. Phys. **2023**, *25*, 2131−2141.
41. Purkayastha, P.; Chattopadhyay, N. Role of rotamerisation and excited state intramolecular proton transfer in the photophysics of 2-(2′-hydroxyphenyl)benzoxazole, 2-(2′-hydroxyphenyl)benzimidazole and 2-(2′-hydroxyphenyl)benzothiazole : a theoretical study. Phys. Chem. Chem. Phys. **2000**, *2*, 203−210.
42. Becke, A.D. A multicenter numerical integration scheme for polyatomic molecules. J. Chem. Phys. **1988**, *88*, 2547–2553.
43. Hirshfeld, F.L. Bonded-Atom Fragments for Describing Molecular Charge Densities. Theoret. Chim. Acta **1977**, *44*, 129–138.
44. Parr, R.G.; Yang, W.T. Density Functional Theory of Atoms and Molecules; Oxford University Press: Oxford, UK, 1989.
45. Teale, A.M.; Helgaker, T.; Savin, A.; Adamo, C.; Aradi, B.; Arbuznikov, A.V.; Ayers, P.W.; Baerends, E.J.; Barone, V.; Calaminici, P.; Cancès, E.; Carter, E.A.; Chattaraj, P.K.; Chermette, H.; Ciofini, I.; Crawford, T.D.; De Proft, F.; Dobson, J.F.; Draxl, C.; Frauenheim, T.; Fromager, E.; Fuentealba, P.; Gagliardi, L.; Galli, G.; Gao, J.L.; Geerlings, P.; Gidopoulos, N.; Gill, P.M.W.; Gori-Giorgi, P.; Görling, A.; Gould, T.; Grimme, S.; Gritsenko, O.; Jensen, H.J.A.; Johnson, E.R.; Jones, R.O.; Kaupp, M.; Köster, A.M.; Kronik, L.; Krylov, A.I.; Kvaal, S.; Laestadius, A.; Levy, M.; Lewin, M.; Liu, S.B.; Loos, P.-F.; Maitra, N.T.; Neese, F.; Perdew, J.P.; Pernal, K.; Pernot, P.; Piecuch, P.; Rebolini, E.; Reining, L.; Romaniello, P.; Ruzsinszky, A.; Salahub, D.R.; Scheffler, M.; Schwerdtfeger, P.; Staroverov, V.N.; Sun, J.W.; Tellgren, E.; Tozer, D.J.; Trickey, S.B.; Ullrich, C.A.; Vela, A.; Vignale, G.; Wesolowski, T.A.; Xu, X.; Yang, W.T. DFT exchange: sharing perspectives on the workhorse of quantum chemistry and materials science. Phys. Chem. Chem. Phys. **2022**, *24*, 28700–28781.
46. Li, S.H.; Li, W.; Fang, T. An Efficient Fragment-Based Approach for Predicting the Ground-State Energies and Structures of Large Molecules. J. Am. Chem. Soc. **2005**, *127*, 7215–7226.
47. Li, W.; Li, S.H.; Jiang, Y.S. Generalized Energy-Based Fragmentation Approach for Computing the Ground-State Energies and Properties of Large Molecules. J. Phys. Chem. A **2007**, *111*, 2193–2199.
48. Li, S.H.; Li, W.; Ma, J. Generalized Energy-Based Fragmentation Approach and Its Applications to Macromolecules and Molecular Aggregates. Acc. Chem. Res. **2014**, *47*, 2712–2720.
49. Li, W.; Dong, H.; Ma, J.; Li, S.H. Structures and Spectroscopic Properties of Large Molecules and Condensed-Phase Systems Predicted by Generalized Energy-Based Fragmentation Approach. Acc. Chem. Res. **2021**, *54*, 169–181.
50. Schwerdtfeger, P.; Nagle, J.K. Table of static dipole polarizabilities of the neutral elements in the periodic table. Mol. Phys. **2018**, *117*, 1200–1225.
51. Shannon, C.E. A mathematical theory of communication. Bell Syst. Tech. J. **1948**, *27*, 379–423.
52. Fisher, R.A. Theory of statistical estimation. Math. Proc. Camb. Philos. Soc. **1925**, *22*, 700–725.
53. Ghosh, S.K.; Berkowitz, M.; Parr, R.G. Transcription of ground-state density-functional theory into a local thermodynamics. Proc. Natl. Acad. Sci. U.S.A. **1984**, *81*, 8028–8031.
54. Bader, R.F.W.; Preston, H.J.T. The kinetic energy of molecular charge distributions and molecular stability. Int. J. Quantum Chem. **1969**, *3*, 327–347.
55. Tal, Y.; Bader, R.F.W. Studies of the energy density functional approach. 1. Kinetic energy. Int. J. Quantum Chem. **1978**, *14*, 153–168.
56. Cohen, L. Local kinetic energy in quantum mechanics. J. Chem. Phys. **1979**, *70*, 788–789.
57. Cohen, L. Representable local kinetic energy. J. Chem. Phys. **1984**, *80*, 4277–4279.
58. Yang, Z.Z.; Liu, S.B.; Wang, Y.A. Uniqueness and Asymptotic Behavior of the Local Kinetic Energy. Chem. Phys. Lett. **1996**, *258*, 30–36.
59. Ayers, P.W.; Parr, R.G.; Nagy,Á. Local kinetic energy and local temperature in the density-functional theory of electronic structure. Int. J. Quantum Chem. **2002**, *90*, 309–326.
60. Anderson, J.S.M.; Ayers, P.W.; Hernandez, J.I.R. How Ambiguous Is the Local Kinetic Energy? J. Phys. Chem. A **2010**, *114*, 8884–8895.
61. Berkowitz, M. Exponential approximation for the density matrix and the Wigner distribution. Chem. Phys. Lett. **1986**, *129*, 486–488.
62. Geerlings, P.; De Proft, F.; Langenaeker, W. Conceptual Density Functional Theory. Chem. Rev. **2003**, *103*, 1793–1873.

 doi:10.20944/preprints202302.0116.v1

63. Johnson, P.A.; Bartolotti, L.J.; Ayers, P.W.; Fievez, T.; Geerlings, P. Charge density and chemical reactivity: A unified view from conceptual DFT. in Modern Charge Density Analysis, ed. Gatti, C. and Macchi, P. Springer, New York, 2012.
64. Liu S.B. Conceptual Density Functional Theory and Some Recent Developments. Acta Phys.-Chim. Sin. **2009**, *25*, 590–600.
65. Geerlings, P.; Chamorro, E.; Chattaraj, P.K.; De Proft, F.; Gázquez, J.L.; Liu, S.B.; Morell, C.; Toro-Labbé, A.; Vela, A.; Ayers, P.W. Conceptual density functional theory: status, prospects, issues. Theor. Chem. Acc. **2020**, *139*, 36.
66. Liu, S.B.; Rong, C.Y.; Wu, Z.M.; Lu, T. Rényi entropy, Tsallis entropy and Onicescu information energy in density functional reactivity theory. Acta Phys.-Chim. Sin. **2015**, *31*, 2057–2063.
67. Kullback, S. Information Theory and Statistics; Dover Publications: Mineola, NY, USA, 1997.
68. Liu, S.B. Identity for Kullback-Leibler divergence in density functional reactivity theory. J. Chem. Phys. **2019**, *151*, 141103.
69. Wang, B.; Zhao, D.B.; Lu, T.; Liu, S.B.; Rong, C.Y. Quantifications and Applications of Relative Fisher Information in Density Functional Theory. J. Phys. Chem. A **2021**, *125*, 3802–3811.
70. Rong, C.Y.; Wang, B.; Zhao, D.B.; Liu, S.B. Information-Theoretic approach in density functional theory and its recent applications to chemical problems. WIREs Comput. Mol. Sci. **2020**, *10*, e1461.
71. Rong, C.Y.; Zhao, D.B.; He, X.; Liu, S.B. Development and Applications of the Density-Based Theory of Chemical Reactivity. J. Phys. Chem. Lett. **2022**, *13*, 11191–11200.
72. Liu, S.B. Homochirality Originates from Handedness of Helices. J. Phys. Chem. Lett. **2020**, *11*, 8690–8696.
73. Liu, S.B. Principle of Chirality Hierarchy in Three-Blade Propeller Systems. J. Phys. Chem. Lett. **2021**, *12*, 8720–8725.
74. Nalewajski, R.F.; Parr, R.G. Information theory, atoms in molecules, and molecular similarity. Proc. Natl. Acad. Sci. U.S.A. **2000**, *97*, 8879–8882.
75. Ayers, P.W. Information Theory, the Shape Function, and the Hirshfeld Atom. Theor. Chem. Acc. **2006**, *115*, 370–378.
76. Parr, R.G.; Ayers, P.W.; Nalewajski, R.F. What Is an Atom in a Molecule? J. Phys. Chem. A **2005**, *109*, 3957–3959.
77. Heidar-Zadeh, F.; Ayers, P.W.; Verstraelen, T.; Vinogradov, I.; Vohringer-Martinez, E.; Bultinck, P. Information-Theoretic Approaches to Atoms-in-Molecules: Hirshfeld Family of Partitioning Schemes. J. Phys. Chem. A **2018**, *122*, 4219–4245.
78. Bader, R.F.W. Atoms in Molecules: A Quantum Theory. Oxford University Press, Oxford, England, 1990.
79. Frisch, M.J.; Trucks, G.W.; Schlegel, H.B.; Scuseria, G.E.; Robb, M.A.; Cheeseman, J.R.; Scalmani, G.; Barone, V.; Petersson, G.A.; Nakatsuji, H.; et al. Gaussian 16 Revision C.01; Gaussian Inc.: Wallingford, CT, USA, 2016.
80. Yanai, T.; Tew, D.; Handy, N. A new hybrid exchange-correlation functional using the Coulomb-attenuating method (CAM-B3LYP). Chem. Phys. Lett. **2004**, *393*, 51–57.
81. McLean, A.D.; Chandler, G.S. Contracted Gaussian-basis sets for molecular calculations. 1. 2nd row atoms, *Z*=11-18. J. Chem. Phys. **1980**, *72*, 5639–5648.
82. Bauernschmitt, R.; Ahlrichs, R. Treatment of electronic excitations within the adiabatic approximation of time dependent density functional theory. Chem. Phys. Lett. **1996**, *256*, 454–464.
83. Furche, F.; Ahlrichs, R. Adiabatic time-dependent density functional methods for excited state properties. J. Chem. Phys. **2002**, *117*, 7433–7447.
84. Liu, J.; Liang, W. Analytical Hessian of electronic excited states in time-dependent density functional theory with Tamm-Dancoff approximation. J. Chem. Phys. **2011**, *135*, 014113.
85. Lu, T.; Chen, F.W. Multiwfn: A multifunctional wavefunction analyzer. J. Comput. Chem. **2012**, *33*, 580–592.